JBC Papers in Press. Published on December 21, 2006 as Manuscript M608126200
The latest version is at http://www.jbc.org/cgi/doi/10.1074/jbc.M608126200

Effect of 4-Hydroxy-2-Nonenal Modification on α-Synuclein Aggregation

Zhijie Qin, Dongmei Hu, Shubo Han¶, Stephen H. Reaney§, Donato A. Di Monte§ and Anthony L. Fink*

From the Department of Chemistry & Biochemistry, University of California, Santa Cruz CA 95064
¶Dept. of Natural Sciences, Fayetteville State University, Fayetteville, NC 28301
§The Parkinson's Institute, 1170 Morse Ave., Sunnyvale, CA 4089

Running title**:** HNE modification of α-synuclein

* Address correspondence to**:** Dr. Anthony L. Fink, Department of Chemistry and Biochemistry, University of California, Santa Cruz, California 95064, USA Fax: 831 459-2935; Phone: 831 459-2915; E-mail: enzyme@cats.ucsc.edu

Several observations have implicated oxidative stress and aggregation of the presynaptic protein α-synuclein in the pathogenesis of PD. α-Synuclein has been shown to have affinity for unsaturated fatty acids and membranes enriched in PUFAs, which are especially sensitive to oxidation under conditions of oxidative stress. One of the most important products of lipid oxidation is 4-hydroxynonenal (HNE), which has been implicated in the pathogenesis of Parkinson's disease. Consequently we investigated the effects of the interaction of HNE with α-synuclein.

Incubation of HNE with α-synuclein at pH 7.4, 37°C resulted in covalent modification of the protein, with up to six HNE molecules incorporated as Michael addition products. FTIR and CD spectra indicated that HNE modification of α-synuclein resulted in a major conformational change involving increased β-sheet. HNE modification of α-synuclein led to inhibition of fibrillation in an HNE-concentration-dependent manner. This inhibition of fibrillation was shown to be due to the formation of soluble oligomers based on SEC HPLC and AFM data. Small-angle X-ray scattering analysis indicated that the HNE-induced oligomers are compact and tightly packed. Treatment with guanidinium chloride (GuHCl) demonstrated that the HNE-induced oligomers were very stable with an extremely slow rate of dissociation. Addition of 5 μM HNE-modified oligomers to primary mesencephalic cultures caused marked neurotoxicity, since the integrity of dopaminergic and GABAergic neurons was reduced by 95% and 85%, respectively. Our observations indicate that HNE-modification of α-synuclein prevents fibrillation but may result in toxic oligomers which could therefore contribute to the demise of neurons subjected to oxidative damage.

Parkinson's disease is the second most common neurodegenerative disorder (after Alzheimer's disease) and affects approximately 1-1.5 % of the US population over age 60. PD symptoms are attributed to the progressive loss of dopaminergic neurons in the substantia nigra. Some surviving nigral dopaminergic neurons contain cytosolic filamentous inclusions known as Lewy bodies (LBs) and Lewy neurites (LNs) (1;2). Several observations have implicated the presynaptic protein α-synuclein in the pathogenesis of PD. α-Synuclein was shown to be a major fibrillar component of LBs and LNs (3), and the production of α-synuclein in transgenic mice (4) or in transgenic flies (5) leads to the motor deficits and neuronal inclusions reminiscent of PD. Point mutations in

α-synuclein, and duplication or triplication of the α-synuclein gene, are associated with early-onset familial PD (6-10), indicating the critical role of α-synuclein aggregation in PD.

α-Synuclein is a small (14 kDa), highly conserved protein that is abundant in various regions of the brain (11), and is intrinsically unstructured, i. e. natively unfolded (12;13). It is clear that membranes play an important role in the function of α-synuclein under both normal and pathological conditions. Affinity of α-synuclein for unsaturated fatty acids and membranes enriched in polyunsaturated fatty acids (PUFAs) has been reported (14-17). Although not yet fully understood, the physiological function of α-synuclein is likely to involve a role in modulating synaptic plasticity (18), presynaptic vesicle pool size, and neurotransmitter release (19-21), as well as vesicle recycling (22). In agreement with these membrane-related functions, the amino acid sequence analysis of human α-synuclein shows seven repeats of 11 residues in the N-terminal half of the molecule, with a consensus sequence of KTKEGV, which is reminiscent of lipid-binding domains of apolipoproteins, and the first five repeats are predicted to form amphiphilic helices (23). α-Synuclein is found in both cytoplasmic and membrane-associated forms. Recently, α-synuclein has been shown to bind to lipid raft-like regions of cells (24). α-Synuclein interacts with liposomes containing phospholipids with acidic head groups *in vitro* (25-29). This interaction causes α-synuclein to undergo a conformational change from an unstructured monomer in solution to an α-helical, membrane-bound protein (23;30;31).

Oxidative stress, in which production of highly reactive oxygen species (ROS) overwhelms antioxidant defenses, has been increasingly implicated in a number of neurodegenerative disorders characterized by deposition of abnormal forms of specific proteins in affected neurons, including PD, Alzheimer's disease, Pick's disease, other Lewy body diseases, amyotrophic lateral sclerosis, and Huntington disease (32-38). ROS induce peroxidation of lipids (cellular membrane lipids or circulating lipoprotein molecules) generating highly reactive aldehydes (39). One of the most important products of lipid peroxidation is the highly reactive aldehyde 4-hydroxynonenal (HNE, structure 1) (40;41), which has been implicated in the pathogenesis of neurodegenerative diseases such as Alzheimer's disease, amyotrophic lateral sclerosis, and Parkinson's disease (33-38;42;43).

In the present work, the effect of HNE on the conformation, aggregation and toxicity of α-synuclein have been investigated. The results indicate that HNE readily reacts with α-synuclein to form covalent adducts, and that the modified α-synuclein does not undergo fibrillation, due to the formation of stable soluble oligomers. These oligomers are toxic to primary cultures of mesencephalic cells.

EXPERIMENTAL PROCEDURES

Chemicals - 4-Hydroxyl nonenal (HNE) was purchased from Cayman Chemical. Nonanal (95%) (nonyl aldehyde) was purchased from Aldrich. Peptone and yeast extract used in the medium were purchased from Difco. All other chemicals were purchased from Fisher or Sigma and were of the highest grade available. The water was doubly deionized.

Expression and Purification of α-synuclein - Human wild type α-synuclein was expressed in the E. coli BL21(DE3) cell line transfected with pRK172 α-synuclein WT plasmid (kind gift of M. Goedert, MRC Cambridge) and purified by a procedure modified from (44). Briefly, the pellet from two liters of cells induced with 0.5 mM isopropyl β-D-thiogalactopyranoside was lysed by sonication at 0°C in 50 mM NaCl, 20 mM Tris-HCl, 0.10 % (v/v) Triton-X100, 0.20 mM phenylmethylsulfonyl fluoride at pH 8.0. The lysis suspension was brought to 30% saturation with ammonium sulfate at 0°C (pellet discarded) followed by 50 % saturation with ammonium sulfate. The resultant pellet was dialyzed against 50 mM NaCl, 20 mM Tris-HCl, pH 7.5, loaded onto a 25 × 130 mm DEAE Sepharose Fast Flow column (Amersham Pharmacia Biotech) equilibrated in the same buffer and eluted with a 50-450 mM NaCl gradient. Fractions containing α-synuclein were dialyzed exhaustively against water, clarified by

centrifugation, and lyophilized for storage at –20 °C. The resultant α-synuclein protein was judged to be >95% pure following SDS-polyacrylamide electrophoresis, gel-filtration and MS analysis.

Protein Sample Preparation - Lyophilized protein was dissolved immediately before use in deionized, purified H_2O and the pH was adjusted to 10±0.5 with 0.1 N NaOH to solubilize any aggregated protein. After 10 min incubation at room temperature, the solution was phosphate-buffered to pH 7.4 (10 mM buffer concentration). The protein concentration was determined using an extinction coefficient of 0.40 mg^{-1} cm^2 at 275 nm.

Interaction of α-synuclein with HNE - Freshly prepared protein solution (2 mg/ml in PBS, pH 7.4) was mixed with a pre-determined amount of HNE solution (10 mg/ml in ethanol) to reach a final molar ratio of 1 (protein): 20 (HNE) and incubated at 37°C over night. The modification of α-synuclein was monitored by electrospray mass spectrometry (ESI MS) as a function of time. Control experiments involved mixing α-synuclein with the same amount of ethanol as added to the sample of HNE. A similar protocol was used to examine the effect of different concentrations of HNE.

Circular Dichroism Measurements - Far-UV Circular dichroism spectra were collected on an AVIV model 62DS spectrophotometer between 250 and 190 nm with a step size of 1.0 nm and averaging time 3 second and collecting 5 repeat scans. The protein concentrations were 1.0 mg/ml. Cuvettes of 0.01 cm path length were used. The background of the corresponding buffers without protein was subtracted for all samples and the data were converted into mean residue ellipticity according to their concentrations and path length.

Thin-film Attenuated Total Reflectance Fourier Transform Infrared Spectroscopy (ATR-FTIR) - FTIR spectra of α-synuclein solutions were recorded using a ThermoNicolet Nexus 670 FTIR spectrophotometer for the amide I region from 1700 to 1600 cm^{-1}. 10 μl of protein solutions of unmodified and HNE modified α-synuclein were applied evenly on the surface of a germanium crystal and dried to form a hydrated thin film using a stream of nitrogen. Background and water vapor subtractions were performed. Curve fitting of the amide I regions (raw spectra) were performed using Gaussian/Lorentzian functions with the software GRAMS (45). Second derivative and Fourier self-deconvoluted spectra were used as a peak position guide for the curve fitting procedure.

Size Exclusion Chromatography - The hydrodynamic size of HNE-modified α-synuclein was measured by size-exclusion chromatography on a BioSep-SEC-S 2000 column (Phenomenex) using a Waters HPLC system. The eluting buffer was 10 mM phosphate buffer at pH 7.4.

SAXS Measurements - Small angle X-ray scattering measurements were performed on Beam line 4-2 at the Stanford Synchrotron Radiation Laboratory (SSRL). The SAXS instrument was configured with a Mo:CB_4 multilayer monochromator, an 18 mm beamstop, and a 218 cm sample-to-detector distance. The fresh prepared samples were centrifuged at 10,000 rpm for 10 minutes before illuminated in the X-ray beam using a PTFE flow-cell with 1.3 mm path length to minimize radiation damage. Data were collected with an accumulation time of 10 minutes at 25°C. Buffer scattering was subtracted, and radii of gyration were calculated using the Guinier approximation.

Stability of HNE-induced oligomers - The HNE-induced oligomers were purified using size exclusion chromatography (Superdex 200, Pharmacia). The purified oligomers (1 mg/ml) were treated with series concentrations of GuHCl for 30 minutes at 25°C, followed by HPLC size exclusion analysis using a G2000 column (TOSOH BIOSCIENCE) on a Waters 2695 HPLC system. The flow rate was set to 0.5 ml/min and the eluted species were monitored at 210 nm and 275 nm concurrently.

Mass spectrometry - HNE-modified α-synuclein was analyzed using ESI MS (MicroMass ZMD, UK). Samples were prepared as follows: the protein solution of HNE-modified α-synuclein was run through a desalting column (Pharmacia, 5 ml) to remove any unreacted 4-hydroxy-2-nonenal. 10 μl of the

protein containing-fraction was then loaded on a mini C8 reverse phase column (Pharmacia). After rinsing with 3 column volumes of H_2O, the protein fraction was eluted by 80% acetonitrile and directly injected into the mass spectrometer.

AFM Measurements - AFM images were collected with a PicoScan LE SPM system (Molecular Imaging, Phoenix, AZ) equipped with Acoustic AC mode (Tapping mode) for *ex-situ* experiments. The magnetically coated probes were 5-7 nm radius with a 2.8 Newton/m spring constant, Type II MAC Levers (Molecular Imaging), were used in MAC mode and oscillated at about 30-kHz resonance frequency under an alternating magnetic field. Triangular cantilevers with 100 kHz resonance Frequency and 2 N/m spring constant, the V-shaped cantilever CSC21/Si3N4/No Al (MikroMasch), were used in tapping mode imaging.

Heights ranging from 0.1 to 100 nm were estimated by section analysis, and lateral sizes were calibrated with standard calibration grid. At least four regions of the mica surface were examined to verify that similar structures existed through the sample. No filter treatment was used to modify the images. SPIP 4.0 (Image Metrology) was used to analyze the height, area and volume distribution of the alpha Synuclein aggregates.

Fibril Formation Assays - Assay solutions contained α-synuclein at a concentration of 1.0 mg/ml (70 μM) in 10 mM Tris-HCl and 0.1 M NaCl, pH 7.4 at 37°C, containing 10 μM ThT as a fibrillation indicator (46). A volume of 120 μl of the mixture was pipetted into a well of a 96-well plate (white plastic, clear bottom), and a 1/8th in. diameter Teflon sphere (McMaster-Carr, Los Angeles) was added for agitation. Each sample was run in quadruplicate. The plates were sealed with Mylar plate sealers (Dynex). The plate was loaded into a fluorescence plate reader (Fluoroskan) and incubated at 37°C with shaking at 600 rpm and a diameter of 1 mm. The fluorescence was measured at 30 min intervals with excitation at 450 nm and emission at 485 nm, with a sampling time of 40 ms. The data from replicate wells were averaged before plotting fluorescence vs. time. The data were fit to a sigmoidal equation (eq 1) using Sigmaplot (47):

$$F = (F_i + m_i t) + (F_f + m_f t)/(1 + \exp[-(t - t_m)/\tau]) \quad (1)$$

where F is the fluorescence intensity and t_m is the time to 50% of maximal fluorescence. The initial baseline during the lag time is described by $F_i + m_i t$. The final baseline after the growth phase has ended is described by $F_f + m_f t$. The apparent rate constant, k_{app}, for the growth of fibrils is given by $1/\tau$, the lag time is calculated as $t_m - 2\tau$, and the amplitude, amp, is given by $F_f - F_i$.

Primary Rat Ventral Mesencephalic Cultures - Cultures were prepared from the ventral mesencephalon of Sprague-Dawley rats (Charles River Laboratories) of 14-days gestation (48). Experimental protocols were in accordance with the NIH guidelines for animal use and were approved by the Institutional Animal Care and Use Committee. Dissected tissues were incubated in calcium-free Hank's Balanced Salt Solution (HBSS) containing trypsin (0.1%, Sigma) and DNase (0.5 mg/ml, Sigma) for 6 min. The trypsinization process was terminated by addition of HBSS containing soybean trypsin inhibitor (0.1 mg/ml, Sigma) and DNase (0.5 mg/ml). Cells were dissociated by gentle trituration using a fire-polished Pasteur pipette and were then centrifuged at 100g for 10 min. The supernatant was discarded and the cells were resuspended in DMEM:F12 medium (HyClone) supplemented with 10% Fetal Bovine Serum (FBS, HyClone). Cultures were plated in 96-well plates coated with poly-D-lysine (100mg/ml, Sigma) at a density of 100,000 cells/well in DMEM:F12 containing 10% FBS, penicillin and streptomycin (Sigma). Cells were exposed starting on day 5 in culture for 48 hrs to 0, 1 or 5 μM of freshly prepared 4-HNE-stabilized α-synuclein oligomer (the concentrations were determined on the basis of the amount of protein used to form the oligomers). Cells were exposed with concentrated stocks for minimal addition of media (final dilution 1:10) to avoid toxicity associated with medium changes.

[^{3}H]Dopamine and [^{3}H]GABA Uptake - For assessment of dopamine uptake, cultures were rinsed with DMEM:F12 containing 1 mM ascorbic acid and incubated for 30 min at 37°C with the same buffer containing 1 mCi/ml [^{3}H]dopamine. Non-specific binding was determined in cultures treated with the dopamine uptake inhibitor mazindol (10 μM). To determine GABA uptake, cultures were washed with uptake buffer composed of DMEM:F12 with 500mM β-alanine and 10mM amino oxyacetic acid to block high affinity glial uptake and enzymatic degradation of GABA, respectively. Subsequently, 1 mCi/ml [^{3}H]GABA in uptake buffer was added to cells and incubated for 30 min at 37°C. For both dopamine and GABA uptake cells were rinsed with phosphate-buffered saline (PBS, pH 7.4), the radioactivity was extracted with Optiphase SuperMix Cocktail and measured using a liquid scintillation counter.

RESULTS

Interaction of a-synuclein with HNE in vitro - Preliminary experiments (data not shown), using mass spectrometry, demonstrated that incubation of HNE with α-synuclein at pH 7.4, 37°C resulted in covalent modification of the protein, and that the amount of HNE incorporated increased with increasing concentration of HNE. Preliminary Thioflavin T assays also revealed that HNE modification of α-synuclein led to inhibition of fibrillation in a concentration-dependent manner.

The modification of α-synuclein with HNE was monitored by ESI MS (Fig. 1). The top spectrum, which is the control (α-synuclein with the same amount of ethanol (3%) as in the samples with HNE), shows a single peak with the expected molecular mass for α-synuclein of 14,460 Da. The subsequent spectra are for α-synuclein treated with increasing concentrations of HNE, and show a series of peaks with increasing mass in units of 156 Da, the molecular mass of HNE, as the HNE concentration increased.

The data in Fig. 1 show that α-synuclein is modified by the covalent addition of up to six HNE molecules as Michael addition products, and that the majority of α-synuclein has 1, 2, or 3 HNE added. With one molar equivalent of HNE close to 50% of the protein was modified by the addition of a single HNE. To demonstrate specificity in the reaction of α-synuclein with HNE we compared its affect with that of the related analog, nonyl aldehyde (nonanal), which lacks the unsaturated bond and hydroxyl of HNE. No evidence for covalent modification was found using MS, and the presence of nonanal did not inhibit fibrillation: in fact, incubation of nonanal with α-synuclein led to rapid amorphous aggregation of the protein (data not shown). No evidence was seen in the MS for

stable advanced lipoxidation end products such as the HNE-Lys-derived 2-pentylpyrrole

As shown in figure 1, we find significant labeling (20-30%) of 70 μM alpha-synuclein by a substoichiometric 50 μM concentration of HNE, and a small amount of labeling is observed with 10 μM HNE (but since this is only 15 mol% of the amount of alpha-synuclein we expect limited labeling). Also, even at 10 μM HNE we see a significant increase in the lag time of alpha-synuclein fibrillation (see below). Thus, we contend that the observed effects of low concentrations of HNE suggest that our observations may be physiologically significant.

Conformational changes of α-synuclein induced by HNE modification - As noted, α-synuclein is a natively unfolded protein. At neutral pH it is calculated to have 24 negative charges (15 of which are localized in the last third of the protein sequence), leading to strong electrostatic repulsion, which contributes to the lack of folding of α-synuclein (13). The effects of HNE modification on the α-synuclein structure were compared with unmodified protein using far-UV CD spectroscopy. As shown in Fig. 2, the spectrum of α-synuclein (solid circles) is typical of an unfolded polypeptide chain, with a minimum in the vicinity of 198 nm, and the absence of characteristic bands in the vicinity of 210-230 nm. In the case of HNE-modified protein, however, a major conformational change was observed based on the decrease in negative ellipticity at 198 nm and an increase in negative ellipticity at 217 nm, indicating the formation of β structure. This may be contrasted with the characteristic formation of α-helical structure on α-synuclein binding to lipid vesicles, and suggests that the conformational change in the present case results from an intrinsic change in the α-synuclein molecules rather than from interaction with the lipid-like HNE.

The conformational changes induced by HNE modification of α-synuclein were further characterized by FTIR, which is more sensitive to β-structure than circular dichroism. Fig. 3 shows the FTIR (amide I region) spectra measured for α-synuclein (Fig. 3A) and the HNE-modified protein (Fig. 3B). The FTIR spectrum of α-synuclein is typical of an unfolded polypeptide, with the main peak at 1650 cm^{-1}. In the spectrum of HNE-modified α-synuclein, however, a new peak appears in the vicinity of 1626 cm^{-1}, which corresponds to β-sheet or extended structure (Fig. 3B). This result is consistent with the circular dichroism data, confirming that HNE modification to α-synuclein results in the formation of β-sheet structure.

Effect of HNE modification of α-synuclein on the fibrillation of α-synuclein - The histological dye Thioflavin T (ThT) is widely used for the detection of amyloid fibrils (46;49). In the presence of fibrils, ThT gives rise to enhanced fluorescence emission at 482 nm, whereas unbound ThT is essentially non-fluorescent at this wavelength. The binding of ThT to α-synuclein fibrils is thus a very convenient method for studying the kinetics of fibril formation. The kinetics of α-synuclein fibrillation usually show a characteristic sigmoidal curve, which is composed of an initial lag phase, a subsequent growth phase, and a final equilibrium phase. Such curves are consistent with a nucleation-dependent polymerization model, in which the lag corresponds to the nucleation phase and the exponential part to fibril growth (elongation).

Time-dependent changes in the ThT fluorescence during the incubation of unmodified and HNE-modified α-synuclein at 37°C are shown in Fig. 4. Unmodified α-synuclein shows typical sigmoidal kinetics of fibrillation with a lag time of 15 hours. The HNE-modified α-synuclein, however, showed no change in ThT fluorescence signal on the measured time scale, indicating that HNE modification of the protein leads to loss of its ability to form fibrils.

Oligomerization of HNE-modified α-synuclein - Whereas the ThT assays provide evidence that the HNE-modified α-synuclein does not form fibrils, data from size-exclusion HPLC (SEC) and AFM show that this is due to the formation of soluble oligomers during incubation at 37°C

(Fig. 5, 6). As shown in Fig. 5, in the SEC monomeric α-synuclein elutes at a retention volume of 8 ml. During incubation with HNE, the oligomer peak appeared at 6 ml. The height of the oligomer peak increased concomitantly with a decrease in monomer peak during continued incubation; ultimately all monomers were converted into the oligomers by 60 hours of incubation. The AFM images are consistent with the presence of monomers (25 Å high) and oligomers (60 Å high) after incubation with HNE, compared to the 120 Å height of the fibrils from unmodified α-synuclein (Fig. 6). Due to interactions with the surface of the mica substrate the heights of the objects in the AFM images are smaller than predicted from the solution properties. The volume of the oligomers in the AFM image is consistent with that from the SAXS data (below).

Small-angle X-ray scattering characterization of HNE modified α-synuclein - The size and shape of HNE-induced oligomers were also analyzed using small angle x-ray scattering. The scattering profiles were obtained for 2 mg/ml HNE-induced oligomers compared to 2 mg/ml of unmodified protein. The Guinier plots of these two species (Fig. 7A) give the *Rg* of HNE induced oligomers 103.5 ± 1.3 Å, compared to the Rg of unmodified protein, which was 41 ± 0.4 Å. In addition, the corresponding Kratky plots (Fig. 7B) show that the HNE induced oligomers give a bell-shaped curve in the very small angle area, indicating that the subunits are compact and tightly packed. In contrast, unmodified α-synuclein shows a curve typical of an unfolded protein.

Stability of HNE-α-synuclein oligomers – The stability of the HNE α-synuclein oligomers was determined using GuHCl to denature the protein and monitored using SEC. The eluting patterns of the oligomers treated with increasing concentrations of GuHCl are shown in Fig. 8. Under the experimental conditions, the unmodified monomers of α-synuclein have an elution volume of 7.5 ml. The HNE-induced oligomers, without GuHCl treatment, show an elution volume of 5.2 ml. With increased concentration of GuHCl, the peaks corresponding to the oligomers shifted to slightly larger elution volume, accompanied by lowed absorbance intensity and increased peak width. This observation indicates that high GuHCl concentrations lead to the formation of slightly smaller oligomers, with wider polydispersity. However, even treated with as high as 6 M of GuHCl, the HNE-induced oligomers did not disassociate into monomers, indicating the high stability of the oligomers and their extremely slow rate of dissociation.

HNE-oligomers are toxic to dopaminergic neurons - Experiments aimed at testing the biological consequences of HNE-induced modification of α-synuclein were performed in primary cultures from the rat ventral mesencephalon. In these mixed cultures that contain dopaminergic as well as non-dopaminergic (e.g. GABAergic) neurons, loss of neuronal integrity was assessed as a decrease in neurotransmitter (dopamine or GABA) uptake (50). When cells were incubated for 48 hrs in the presence of 1 μM HNE-modified oligomers, no significant loss of neuronal integrity was observed. However, at a higher concentration (5 μM), these α-synuclein oligomers displayed marked neurotoxicity and caused a 95% and 85% loss of dopaminergic and GABAergic neurons, respectively (Fig. 9).

DISCUSSION

α-synuclein forms covalent adducts with HNE. The roles of 4-hydroxy-2-nonenal in physiology and pathology have been well documented (51). Essentially HNE exhibits a high activity towards thiol and amino groups and the ensuing modified proteins are responsible for most of the biochemical effects. Reactions of the HNE C=C double bond include Michael additions by which HNE-cysteine, HNE-histidine, and HNE-lysine adducts can be formed. Reactions of the aldehyde group could also be involved in some protein modifications, leading to Schiff bases. The mass spectrometry data presented in this work show that the products from the modification of α-synuclein with HNE have the formula of [α-synuclein (14,460 Da) + (HNE (156 Da))$_n$] (n = 1, 2, 3…), indicating the products are the adducts of α-synuclein with increasing numbers of HNE (156 Da) molecules. This indicates that the covalent modification

occurs via Michael addition. The most likely attacking nucleophiles are the side chains of Lys and His. α-Synuclein has a single His residue at position 50, whereas it has 15 Lys residues. It has recently been reported that HNE can modify α-synuclein at His50 (14). Our data indicate that it must also be modified at several of the Lys residues. We also examined the interaction of α-synuclein with nonyl aldehyde, a 9-carbon aldehyde analogue of HNE but without the C=C bond. No evidence for covalent modification to α-synuclein was observed in mass spectrometry analysis after incubation of α-synuclein with nonyl aldehyde. These data are consistent with adduct formation of HNE via Michael addition to the C=C bond.

The fact that significant labeling of alpha-synuclein occurs with low micromolar concentrations of HNE and that such low concentrations of HNE cause a significant increase in the lag time of alpha-synuclein fibrillation suggest that our observations are likely to be physiologically significant.

The HNE-modification of α-synuclein results in conformational changes and oligomerization – Biophysical characterization of the HNE-modified α-synuclein indicate a substantially increased amount of β-sheet; this probably arises from the increased hydrophobicity of the modified protein resulting in partial folding of α-synuclein due to formation of a hydrophobic core. The putative contiguous hydrophobic surface area in this partially folded conformation favors self-association, leading to the observed formation of soluble oligomers. The Kratky plot of the small-angle X-ray scattering data reveals that the subunits in the oligomers are also significantly more compact than the unmodified form of α-synuclein. The marked stability of these oligomers in the presence of high concentrations of GuHCl indicate that the intermolecular interactions in the oligomers are very strong, probably due to a combination of hydrophobic, electrostatic and H-bonding interactions.

Since HNE can cause crosslinking of proteins an alternative possibility is that the very stable oligomers are due to covalent crosslinking between α-synuclein molecules. However, if there were such covalent cross-linking then SDS PAGE should show a series of oligomers. Since we did not see any indication of covalent cross-linking in the HNE-induced stable oligomers by SDS PAGE we can eliminate this possibility.

The increased R_g of the oligomers in the SAXS experiments compared to that of the monomers suggests that the minimum number of subunits of α-synuclein in the oligomers is 16. We ascribe the polydispersity of the oligomers as follows: we believe there is a minimum sized oligomer building block, perhaps an octamer, which readily self-associates to form larger oligomers.

The fact that the HNE oligomers are so stable probably accounts for the lack of fibrillation of the HNE-modified α-synuclein: the protein is tied up in the oligomers, and dissociation is sufficiently slow that negligible α-synuclein monomer builds up. It is also possible that the modification of the α-synuclein side chains by the HNE, and the ensuing increased hydrophobicity and conformational change, lead to disfavored fibrillation and more favored oligomer formation, i. e. kinetics competition favoring the oligomers.

One major implication of the inhibited fibrillation is that, if significant HNE modification of α-synuclein takes place within cells, fibrillation would not occur but rather there would be a buildup of the soluble oligomers. How reasonable is it to hypothesize that this series of events may actually occur within dopaminergic neurons, i.e. the neurons that are preferentially targeted by the neurodegenerative process of Parkinson's disease (PD)? Because of their dopamine content and the ability of dopamine to participate in oxidative reactions, dopaminergic neurons are thought to be particularly prone to oxidative stress (52). This oxidative stress could in turn lead to lipid peroxidation and ultimately to HNE formation. There are several reports suggesting increased HNE modification in Parkinson's disease (43;53;54). Since α-synuclein in its normal physiological situation is bound to membranes containing substantial

unsaturated fatty acyl chains it will inevitably be exposed to significant amounts of HNE, so these observations are consistent with a potentially toxic effect of HNE modification of α-synuclein. Quite interestingly, lipid peroxidation has been reported to be enhanced in the substantia nigra (the area of the brain mostly affected by dopaminergic cell degeneration in PD) of PD patients (55), further supporting the possibility of increased HNE production within dopaminergic cells under pathological conditions. Another intriguing scenario is provided by studies in animal models of PD. Toxicant challenges that induce selective degeneration of dopaminergic neurons are characterized by oxidative stress and HNE formation that occur at the same time when levels of α-synuclein are also up-regulated (56;57). Thus, it appears that, after toxic insults, HNE-mediated modifications of α-synuclein would be facilitated by the concomitant elevation of HNE and α-synuclein levels within dopaminergic neurons. In a previous study, addition of oligomers obtained from human α-synuclein to ventral mesencephalic cultures was linked to neurotoxicity toward dopaminergic neurons (58). Our initial findings concerning the biological effects of HNE-modified oligomers also show that, when added to these cultures, they cause a marked loss of neuronal integrity. Although the precise mechanisms underlying this effect are presently unknown, data support the interpretation that HNE-modified oligomers are potentially toxic and could therefore contribute to the demise of neurons subjected to oxidative damage. In addition, it is important to note that the HNE-modified α-synuclein oligomers may have different pathological effects compared to oligomers formed from unmodified α-synuclein, since it is clear that both types of oligomers have significantly different structures and stabilities.

REFERENCES

1. Forno, L. S. (1996) *J. Neuropathol. Exp. Neurol.* **55,** 259-272

2. Lewy, F. H. (1912) Paralysis Agitans. Pathologische Anatomie. In Lewandowski, M., editor. *Handbuch der Neurologie*, Springer, Berlin

3. Spillantini, M. G., Schmidt, M. L., Lee, V. M. Y., Trojanowski, J. Q., Jakes, R., and Goedert, M. (1997) *Nature* **388,** 839-840

4. Masliah, E., Rockenstein, E., Veinbergs, I., Mallory, M., Hashimoto, M., Takeda, A., Sagara, Y., Sisk, A., and Mucke, L. (2000) *Science* **287,** 1265-1269

5. Feany, M. B. and Bender, W. W. (2000) *Nature* **404,** 394-398

6. Kruger, R., Kuhn, W., Muller, T., Woitalla, D., Graeber, M., Kosel, S., Przuntek, H., Epplen, J. T., Schols, L., and Riess, O. (1998) *Nat. Genet.* **18,** 106-108

7. Polymeropoulos, M. H., Lavedan, C., Leroy, E., Ide, S. E., Dehejia, A., Dutra, A., Pike, B., Root, H., Rubenstein, J., Boyer, R., Stenroos, E. S., Chandrasekharappa, S., Athanassiadou, A., Papapetropoulos, T., Johnson, W. G., Lazzarini, A. M., Duvoisin, R. C., Di Iorio, G., Golbe, L. I., and Nussbaum, R. L. (1997) *Science* **276,** 2045-7

8. Zarranz, J. J., Alegre, J., Gomez-Esteban, J. C., Lezcano, E., Ros, R., Ampuero, I., Vidal, L., Hoenicka, J., Rodriguez, O., Atares, B., Llorens, V., Gomez, T. E., del Ser, T., Munoz, D. G., and de Yebenes, J. G. (2004) *Ann. Neurol.* **55,** 164-173

9. Trojanowski, J. Q. and Lee, V. M. (2003) *Ann. N. Y. Acad. Sci.* **991,** 107-110

10. Singleton, A. B., Farrer, M., Johnson, J., Singleton, A., Hague, S., Kachergus, J., Hulihan, M., Peuralinna, T., Dutra, A., Nussbaum, R., Lincoln, S., Crawley, A., Hanson, M., Maraganore, D., Adler, C., Cookson, M. R., Muenter, M., Baptista, M., Miller, D., Blancato, J., Hardy, J., and Gwinn-Hardy, K. (2003) *Science* **302,** 841

11. Maroteaux, L., Campanelli, J. T., and Scheller, R. H. (1988) *J Neurosci* **8,** 2804-15

12. Weinreb, P. H., Zhen, W., Poon, A. W., Conway, K. A., and Lansbury, P. T., Jr. (1996) *Biochemistry* **35,** 13709-13715

13. Uversky, V. N., Gillespie, J. R., and Fink, A. L. (2000) *Proteins* **41,** 415-427

14. Trostchansky, A., Lind, S., Hodara, R., Oe, T., Blair, I. A., Ischiropoulos, H., Rubbo, H., and Souza, J. M. (2006) *Biochem. J.* **393,** 343-349

15. Sharon, R., Bar-Joseph, I., Frosch, M. P., Walsh, D. M., Hamilton, J. A., and Selkoe, D. J. (2003) *Neuron* **37,** 583-595

16. Sharon, R., Bar-Joseph, I., Mirick, G. E., Serhan, C. N., and Selkoe, D. J. (2003) *J Biol. Chem* **278,** 49874-49881

17. Perrin, R. J., Woods, W. S., Clayton, D. F., and George, J. M. (2001) *J. Biol. Chem.* **276,** 41958-41962

18. George, J. M., Jin, H., Woods, W. S., and Clayton, D. F. (1995) *Neuron* **15,** 361-372

19. Cabin, D. E., Shimazu, K., Murphy, D., Cole, N. B., Gottschalk, W., McIlwain, K. L., Orrison, B., Chen, A., Ellis, C. E., Paylor, R., Lu, B., and Nussbaum, R. L. (2002) *J. Neurosci.* **22,** 8797-8807

20. Abeliovich, A., Schmitz, Y., Farinas, I., Choi-Lundberg, D., Ho, W. H., Castillo, P. E., Shinsky, N., Verdugo, J. M., Armanini, M., Ryan, A., Hynes, M., Phillips, H., Sulzer, D., and Rosenthal, A. (2000) *Neuron* **25,** 239-252

21. Murphy, D. D., Rueter, S. M., Trojanowski, J. Q., and Lee, V. M. (2000) *J. Neurosci.* **20,** 3214-3220

22. Lotharius, J. and Brundin, P. (2002) *Hum. Mol. Genet.* **11,** 2395-2407

23. Davidson, W. S., Jonas, A., Clayton, D. F., and George, J. M. (1998) *J. Biol. Chem.* **273,** 9443-9449

24. Fortin, D. L., Troyer, M. D., Nakamura, K., Kubo, S., Anthony, M. D., and Edwards, R. H. (2004) *J. Neurosci.* **24,** 6715-6723

25. Cole, R. N. and Hart, G. W. (2001) *J. Neurochem.* **79,** 1080-1089

26. Narayanan, V. and Scarlata, S. (2001) *Biochemistry* **40,** 9927-9934

27. McLean, P. J., Kawamata, H., Ribich, S., and Hyman, B. T. (2000) *J. Biol. Chem.* **275,** 8812-8816

28. Sharon, R., Goldberg, M. S., Bar-Josef, I., Betensky, R. A., Shen, J., and Selkoe, D. J. (2001) *Proc. Natl. Acad. Sci. U. S. A* **98,** 9110-9115

29. Zhu, M., Li, J., and Fink, A. L. (2003) *J Biol Chem* **278,** 40186-40197

30. Eliezer, D., Kutluay, E., Bussell, R., Jr., and Browne, G. (2001) *J. Mol. Biol.* **307,** 1061-1073

31. Zhu, M. and Fink, A. L. (2003) *J Biol Chem* **278,** 16873-16877

32. Wang, D. S., Iwata, N., Hama, E., Saido, T. C., and Dickson, D. W. (2003) *Biochem. Biophys. Res. Commun.* **310,** 236-241

33. Zarkovic, K. (2003) *Mol. Aspects Med.* **24,** 293-303

34. Markesbery, W. R. (1999) *Archives of Neurology* **56,** 1449-1452

35. Jenner, P. (2003) *Ann. Neurol.* **53 Suppl 3,** S26-S36

36. Lev, N. and Melamed, E. (2001) *Isr. Med. Assoc. J.* **3,** 435-438

37. Gerst, J. L., Siedlak, S. L., Nunomura, A., Castellani, R., Perry, G., and Smith, M. A. (1999) *Dement. Geriatr. Cogn Disord.* **10 Suppl 1,** 85-87

38. Ferrante, R. J., Browne, S. E., Shinobu, L. A., Bowling, A. C., Baik, M. J., MacGarvey, U., Kowall, N. W., Brown, R. H., Jr., and Beal, M. F. (1997) *J. Neurochem.* **69,** 2064-2074

39. Esterbauer, H., Schaur, R. J., and Zollner, H. (1991) *Free Radic. Biol. Med.* **11,** 81-128

40. Yoritaka A., Hattori N, Uchida K., Tanaka M., Stadtman E.R, and Mizuno Y. (1996) *Proc. Natl. Acad. Sci. U. S. A* **93,** 2696-2701

41. Uchida, K. and Stadtman, E. R. (1992) *Proc. Natl. Acad. Sci. U. S. A* **89,** 4544-4548

42. Smith, M. P. and Cass, W. A. (2006) *Neuroscience*

43. Dalfo, E., Portero-Otin, M., Ayala, V., Martinez, A., Pamplona, R., and Ferrer, I. (2005) *J. Neuropathol. Exp. Neurol.* **64,** 816-830

44. Conway, K. A., Harper, J. D., and Lansbury, P. T. (1998) *Nature Medicine* **4,** 1318-1320

45. Fink, A. L., Seshadri, S., Khurana, R., and Oberg, K. A. (1999) Determination of Secondary Structure in Protein Aggregates Using Attenuated Total Reflectance (ATR) FTIR. In B.R.Singh, editor. *Infrared Analysis of Peptides and Proteins*, Amer. Chemical Society, NY

46. Naiki, H., Higuchi, K., Hosokawa, M., and Takeda, T. (1989) *Analytical Biochemistry* **177,** 244-249

47. Nielsen, L., Khurana, R., Coats, A., Frokjaer, S., Brange, J., Vyas, S., Uversky, V. N., and Fink, A. L. (2001) *Biochemistry* **40,** 6036-6046

48. Shimoda, K., Sauve, Y., Marini, A., Schwartz, J. P., and Commissiong, J. W. (1992) *Brain Res.* **586,** 319-331

49. LeVine, H., III (1993) *Protein Sci.* **2,** 404-410

50. Driscoll, B. F., Law, M. J., and Crane, A. M. (1991) *J. Neurochem.* **56,** 1201-1206

51. Dianzani, M. U. (2003) *Mol. Aspects Med.* **24,** 263-272

52. Dauer, W. and Przedborski, S. (2003) *Neuron* **39,** 889-909

53. Sajadi, A., Bensadoun, J. C., Schneider, B. L., Lo, B. C., and Aebischer, P. (2006) *Neurobiol. Dis.* **22,** 119-129

54. Smith, M. P. and Cass, W. A. (2006) *Neuroscience*

55. Dexter, D. T., Carter, C. J., Wells, F. R., Javoy-Agid, F., Agid, Y., Lees, A., Jenner, P., and Marsden, C. D. (1989) *J. Neurochem.* **52,** 381-389

56. Manning-Bog, A. B., McCormack, A. L., Li, J., Uversky, V. N., Fink, A. L., and Di Monte, D. A. (2002) *J. Biol. Chem.* **277,** 1641-1644

57. McCormack, A. L., Atienza, J. G., Johnston, L. C., Andersen, J. K., Vu, S., and Di Monte, D. A. (2005) *J. Neurochem.* **93,** 1030-1037

58. Zhang, W., Wang, T., Pei, Z., Miller, D. S., Wu, X., Block, M. L., Wilson, B., Zhang, W., Zhou, Y., Hong, J. S., and Zhang, J. (2005) *FASEB J.* **19,** 533-542

FIGURE LEGENDS

Figure 1. Molecular mass of HNE modified α-synuclein determined by ESI-MS. Unmodified α-synuclein gives a mass of 14,460 Da as shown in the top spectrum. Reaction with increasing concentrations of HNE (10, 50, 100, 500 2000 μM) gives spectra with multiple peaks corresponding to the formation of adducts with increasing numbers of HNE molecules. Each larger peak is exactly 156 Da higher than the preceding one.

Figure 2. Comparison of secondary structure changes induced by HNE-modification of α-synuclein. Far-UV circular dichroism showing HNE-modified α-synuclein (open circles) and unmodified α-synuclein (solid circles). Spectra were collected with protein concentrations of 70 μM in 10 mM phosphate buffer, pH 7.4, 25 °C, 0.1 mm path length.

Figure 3. Amide I region of the FTIR spectra of unmodified α-synuclein (A) and HNE-modified α-synuclein (B). The solid lines represent the raw ATR-FTIR spectra and the dash lines represent the curve-fitted components used for secondary structure analysis (see Methods). The HNE-mod α-synuclein shows substantially more β-sheet structure (1623 cm^{-1}).

Figure 4. Kinetics of the aggregation of unmodified (Δ) and HNE-modified (○) α-synuclein monitored by thioflavin T fluorescence. The solutions contained 70 μM α-synuclein, 37 °C, and were stirred 600 rpm in pH 7.4 phosphate buffer with 100 mM NaCl.

Figure 5. The formation of oligomers on incubation of HNE-modify α-synuclein, monitored by SEC-HPLC. Separation was achieved with a TSK S2000 column eluting with a 0.5 ml/min pH 7.4 phosphate buffer. Unmodified α-synuclein has a retention volume of 8 ml. The traces were accumulated over a 60 h period, as indicated, from top to bottom.

Figure 6. AFM images of representative unmodified and HNE-modified α-synuclein after incubation as described in methods. A: Typical fibrils formed from unmodified α-synuclein. B: Oligomers and monomers formed from HNE-modified α-synuclein after incubation for 60 hours.

Figure 7. Small angle X-ray scattering (SAXS) data for HNE-modified α-synuclein compared with the unmodified protein. A: Represent Guinier plots, from which the radius of gyration (Rg) was estimated (open circles and solid circles represent HNE-modified and unmodified protein respectively). B shows Kratky plots of HNE-modified (solid line) and unmodified type protein (dotted line). The bell-shaped curve for the HNE-modified protein indicates that it is tightly packed, in contrast to the unfolded unmodified protein.

Figure 8. HNE-modified α-synuclein oligomers are stable to GuHCl. SEC HPLC traces show the effect of increasing concentration of GuHCl from 0 to 6 M on the oligomers. The solid line shows the peak for monomeric α-synuclein. Even in 6 M GuHCl no monomer is formed.

Figure 9. Effect of HNE-modified α-synuclein oligomers on the integrity of neurons in culture. Primary cultures from the rat ventral mesencephalon were incubated for 48 hrs in the presence of vehicle (control) or HNE-modified α-synuclein oligomers. Loss of neuronal integrity was measured as a decrease in dopamine (dark bars) or GABA (empty bars) uptake. Bar represents the mean ± SEM of measurements in 6 separate wells. Data were analyzed by two-way ANOVA and Tukey's post-hoc analysis. *Statistically different from the corresponding (dopamine vs. GABA) control ($p < 0.001$).

Structure 1 (Qin et al)

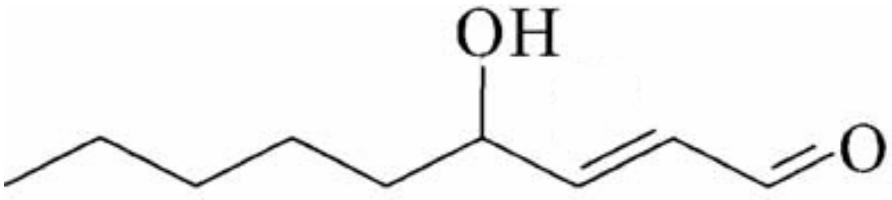

Figure 1. (Qin et al)

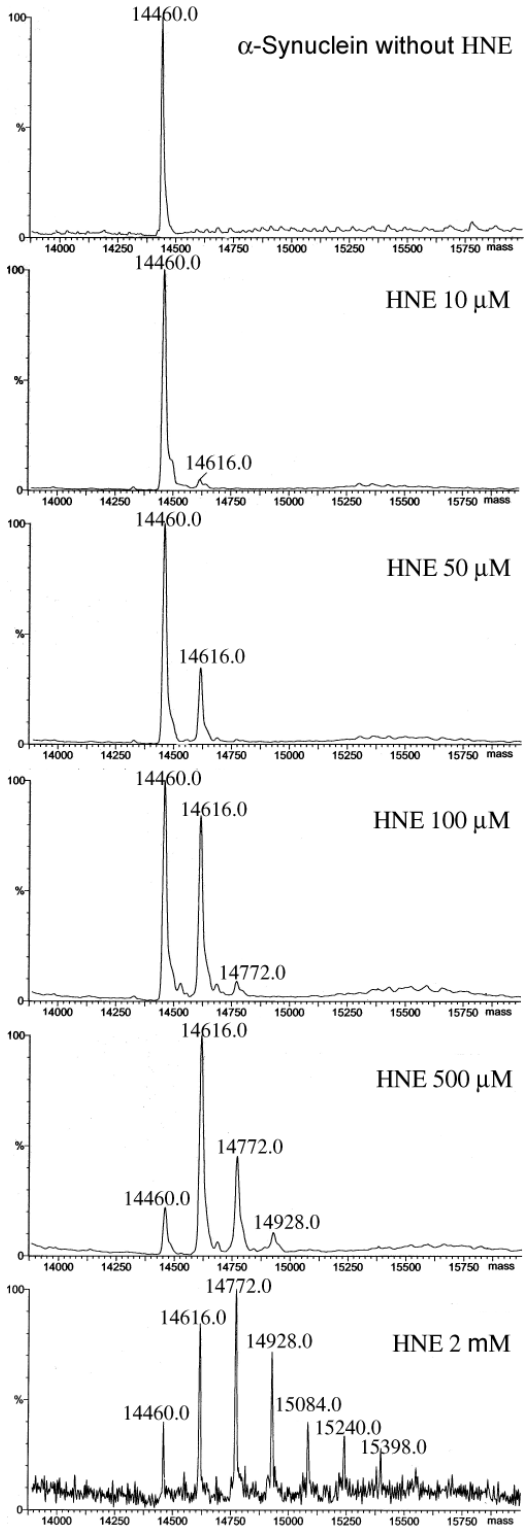

Figure 2. (Qin et al)

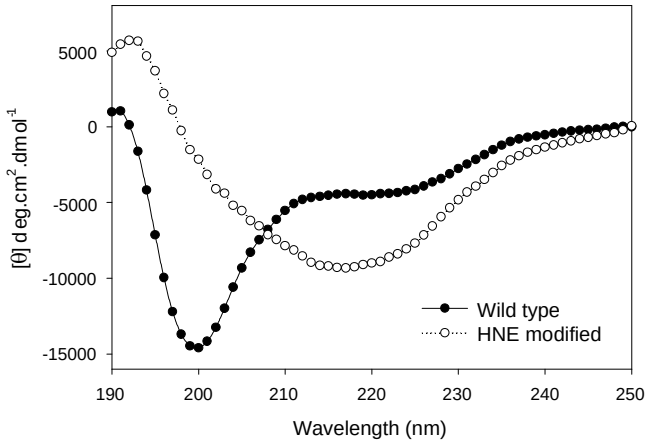

Figure 3. (Qin et al)

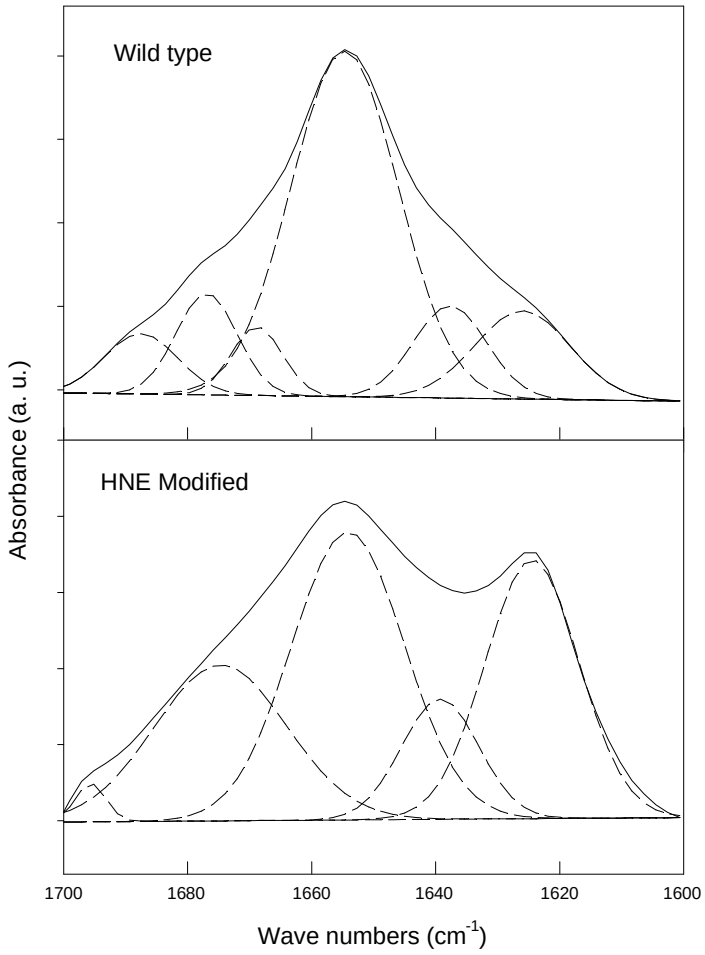

Figure 4. (Qin et al)

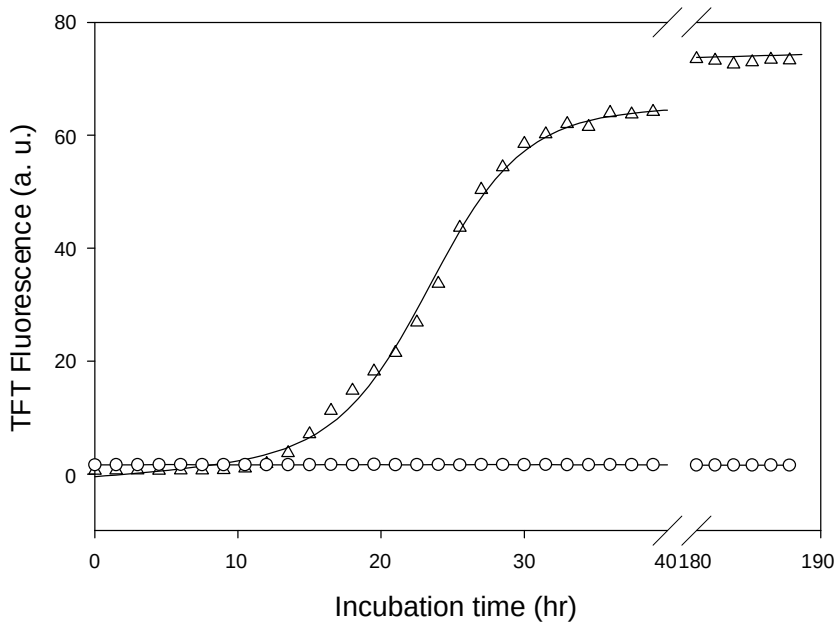

Figure 5. (Qin et al)

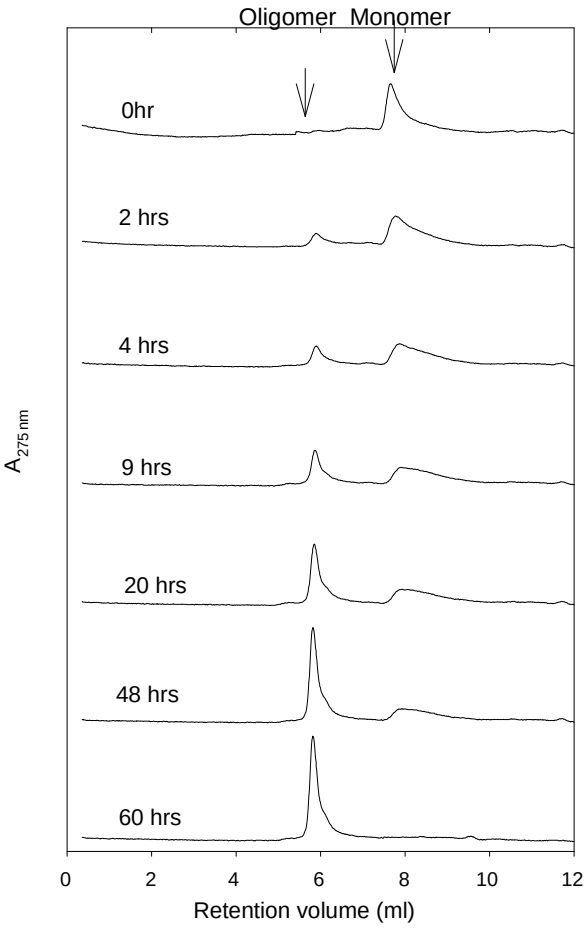

Figure 6. (Qin et al.)

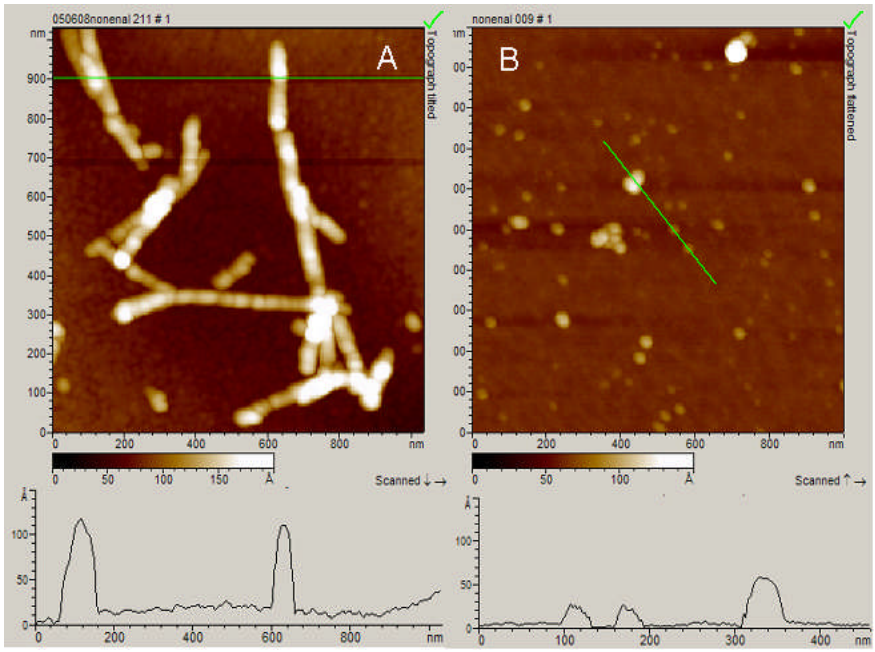

Figure 7. (Qin et al.)

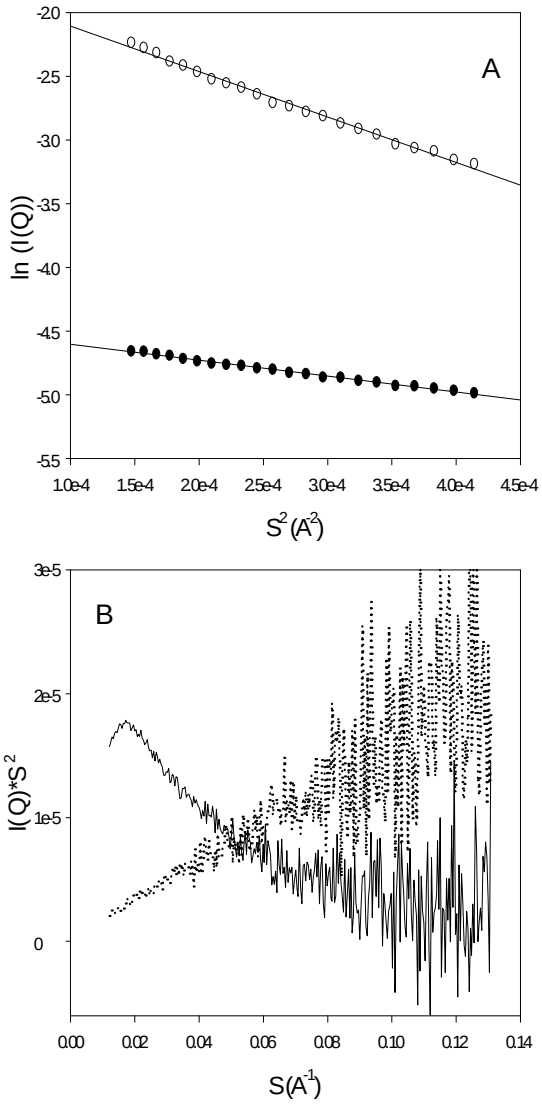

Figure 8. (Qin et al.)

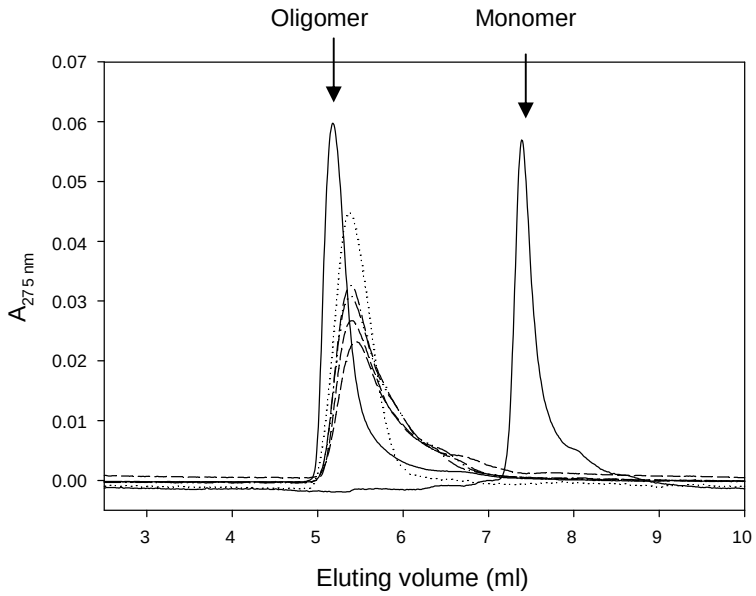

Figure 9. (Qin et al.)

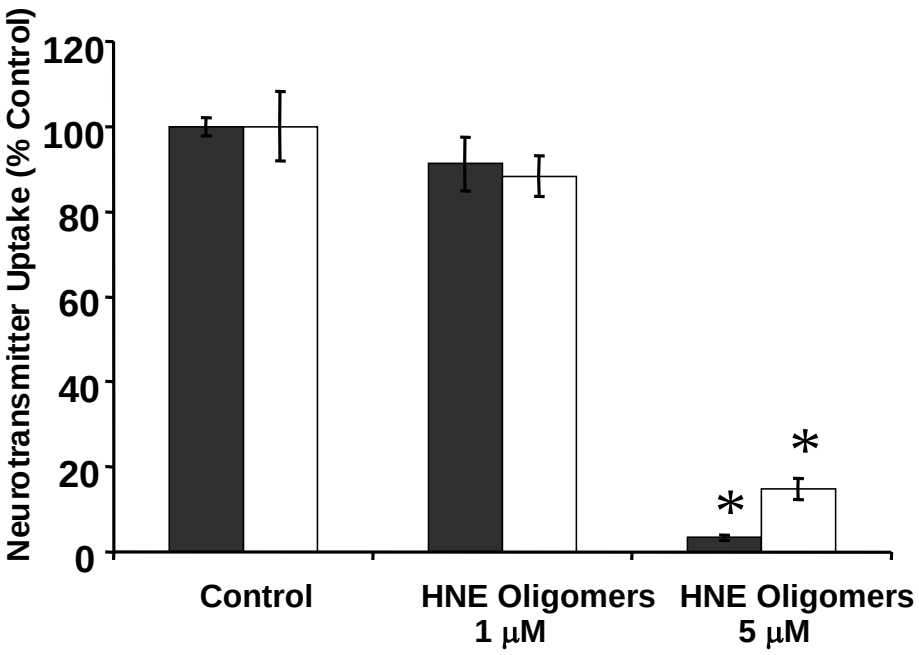

Effect of 4-hydroxy-2-nonenal modification on α-synuclein aggregation

Zhijie Qin, Dongmei Hu, Shubo Han, Stephen H. Reaney, Donato A. Di Monte and Anthony L. Fink

J. Biol. Chem. published online December 21, 2006
